

Polarization Analyses of Readout Signals in Phase Change Material

Incorporating a Solid Immersion Lens (SIL)

Chung-Hao Tien, Yin-Chieh Lai, Han-Ping D. Shieh
Institute of Electro-Optical Engineering, National Chiao Tung University
Hsin-Chu, Taiwan, 30010, Rep. of China
Tel: 886-3-5726111-59211 Fax: 886-3-5737681 Email: u8624503@cc.nctu.edu.tw

ABSTRACT

Comprehensive analyses based on rigorous vector diffraction theory have been presented to simulate the readout signal contrast using SIL in reading phase change recording disk. De-polarized reflected light (y-polarized from x-polarized incident beam) results in the reduction of total signal contrast, and becomes more obvious for high numerical aperture (NA) systems. Due to the signal degradation from de-polarized reflected light, filtering de-polarized light is applied to signal detection. The x-polarized contrast is a factor 1.0 to 1.35 higher than the conventional detection contrast (x+y polarized) at different gap widths, at a cost of 0 to 25 percent total intensity reduction.

Keywords: Solid Immersion Lens (SIL), near-field recording, NA (numerical aperture), polarization, vector diffraction.

INTRODUCTION

Areal density of optical recording is limited by the laws of diffraction to be about $0.6\lambda/NA$, where λ is the wavelength of the laser and NA is the numerical aperture of the focusing lens. A solid immersion lens (SIL) attached to an objective with effective NA higher than 1 is a feasible scheme to produce an ultra-small focus laser spot to read/write in optical recording¹⁻⁴. The principle of the SIL-based near field optics is that by focusing light inside a high refraction index lens without another refraction, the wavelength of light is shrunk by a factor n , where n is the refraction index of the lens. Based on vector diffraction theory using plane-wave expansion, the spectrum within the critical angle of SIL-air interface will diffract like a focus wave with $NA=1$ (region1), the other part will decay exponentially away from the bottom of SIL (region2). When the SIL was positioned closely enough to the disk, optical tunneling effect of region2 results in increasing the effective numerical aperture (NA) above theoretical upper limit of 1 in air⁵. Through evanescent coupling into the recording medium, the reduced marks can be readout using SIL, promising substantial increase in the storage density. For SIL systems with $NA_{\text{eff}} > 1$, the air gap spacing between SIL lens and recording medium dramatically affects the signal contrast. Moreover, in such high NA systems, the incident angle is so large that the readout signal will be affected by de-

polarization effect. Here we examine the effect of de-polarization on readout signal contrast in phase change disks using SIL.

SYSTEM LAYOUT

The SIL-based system and disk structures are shown in Fig. 1. We adopt the linearly x-polarized Gaussian beam with a $1/e$ radius of $r_0=RA$ (the objective radius), resulting in an effective $NA_{\text{eff}}=1.1$ and 1.48 for 0.6-NA and 0.8-NA objective lens with SIL ($n=2.0$), respectively. Reflected beam is collimated, separated into the x and y-polarized electric field by a PBS and then detected denoted by S_1 and S_2 , respectively. The full vectorial character of light is considered in this simulation. Here reflective crystalline and amorphous state in x-polarized is denoted as S_{1X} and S_{1A} , respectively, while S_{2x} and S_{2A} for y-polarized, respectively. The readout signal contrast is defined as $(S_{1X}-S_{1A})^2 / (S_{1X}+S_{1A})$.

SIMULATION METHODS

Our approach to vector diffraction is based on Mansuripur's^{6,7}. Wavefront is decomposed into a set of plane waves that propagate independently through the SIL system. Then each plane wave propagation in θ and ϕ directions has associated with its two orthogonal electric fields in the input pupil plane, E_p^0 and E_s^0 , which are aligned in the radial and azimuthal directions, respectively. After reflected from the layered media, the two independent electric fields become E_p and E_s . The reflection matrix of the phase-change disk can be written as follows:

$$\begin{bmatrix} E_p \\ E_s \end{bmatrix} = \begin{bmatrix} R_{pp} & R_{ps} \\ R_{sp} & R_{ss} \end{bmatrix} \begin{bmatrix} E_p^0 \\ E_s^0 \end{bmatrix} \quad (1)$$

$$\theta = \tan^{-1} \left(\frac{\sqrt{E_x^2 + E_y^2}}{E_z} \right) \quad \phi = \tan^{-1} \frac{E_y}{E_x}$$

The reflection coefficient given by thin-film matrix techniques is adopted for reflected field at the medium. In phase change material, s and p-polarized waves are independent as the cross terms R_{ps} and R_{sp} are zero. After coordinate transformation, the polarization of a refracted beam can be expressed in terms of that of the incident beams in Cartesian coordinates:

$$\begin{bmatrix} E_x \\ E_y \\ E_z \end{bmatrix} = \begin{bmatrix} \Psi_{xx} & \Psi_{xy} \\ \Psi_{yx} & \Psi_{yy} \\ \Psi_{zx} & \Psi_{zy} \end{bmatrix} \begin{bmatrix} E_x^0 \\ E_y^0 \end{bmatrix} \quad (2)$$

where

$$\begin{aligned} \Psi_{xx} &= \frac{1}{2} \left\{ (R_{ss} + R_{pp} \cos \theta) - (R_{ss} - R_{pp} \cos \theta) \cos 2\phi - (R_{sp} + R_{ps} \cos \theta) \sin 2\phi \right\} \\ \Psi_{xy} &= \frac{1}{2} \left\{ (R_{sp} - R_{ps} \cos \theta) - (R_{sp} + R_{ps} \cos \theta) \cos 2\phi + (R_{ss} - R_{pp} \cos \theta) \sin 2\phi \right\} \\ \Psi_{yx} &= \frac{1}{2} \left\{ (R_{sp} - R_{ps} \cos \theta) + (R_{sp} + R_{ps} \cos \theta) \cos 2\phi - (R_{ss} - R_{pp} \cos \theta) \sin 2\phi \right\} \\ \Psi_{yy} &= \frac{1}{2} \left\{ (R_{ss} + R_{pp} \cos \theta) + (R_{ss} - R_{pp} \cos \theta) \cos 2\phi + (R_{sp} + R_{ps} \cos \theta) \sin 2\phi \right\} \\ \Psi_{zx} &= (R_{pp} \cos \phi - R_{ps} \sin \phi) \sin \theta \\ \Psi_{zy} &= (R_{ps} \cos \phi + R_{pp} \sin \phi) \sin \theta \end{aligned}$$

At a focal length from the SIL bottom along the z axis, the electric field distribution in exit pupil is obtained by superimposing each plane waves, taking into account their different propagation paths and polarization vectors. The integral of the overall electric field can be computed efficiently by fast-Fourier-transform (FFT) algorithm. Finally, the reflected electric field components of x and y polarized (z is too small to be included) separated by PBS are detected individually.

SIMULATION RESULTS

The difference and DC values of reflected wave in x and y-polarized for $NA_{\text{eff}}=1.1$ are shown in Fig. 2(a). DC values of x-polarized $S_{1X}-S_{1A}$ change extensively as the gap width increases, which mainly determine the signal contrast, as shown in Fig. 2(b). On the other hand, the y-polarized $S_{2X}+S_{2A}$ is so weak that the signal contrast degradation due to y-polarized can be neglected. Moreover, the contrast of y-polarized is even reversed at gap width ≈ 0 nm because of interference effects.

Then we use an annular aperture, shown in Fig. 1, to block the rays below the critical total reflection angle (TIR) angle to concentrate on the readout contrast of evanescent wave, as shown in Figs. 3(a) and (b), respectively. The ratio of block radius to full aperture radius is 0.77. As shown in Fig. 3(a), the DC values of both x ($S_{1X}+S_{1A}$) and y-polarized ($S_{2X}+S_{2A}$) increase as air-gap increases because of the total reflection effect. As the air-gap exceeds about 400 nm, the incident beam is all reflected by TIR so that the signal contrast in both x and y-polarized approach to zero, as shown in Fig. 3(b).

De-polarization resulted from large incident angle becomes more significant in higher NA systems. Then, we used a $NA_{\text{eff}}=1.48$ to examine the relationship between polarized readout contrast and gap width compared to $NA_{\text{eff}}=1.1$. As Fig. 4(a) shows, DC values of y-polarized ($S_{2X}+S_{2A}$) increase compared to $NA_{\text{eff}}=1.1$, shown in Fig. 2(a), result in apparent degradation of total contrast due to y-polarized, as shown in Fig. 4(b).

We also observed the annular aperture of $NA_{\text{eff}}=1.48$, compared with $NA_{\text{eff}}=1.1$, to observe whether more evanescent components have influence on readout signal contrast. The ratio of block radius to full aperture radius is 0.44. As Fig. 5(a) shows, the signal and DC values both increase compared to $NA_{\text{eff}}=1.1$. Consequently, the total readout contrast will not be

improved by more evanescent components, as shown in Fig. 5(b). Moreover, the faster decay of evanescent wave results in contrast margin shrunk when gap is below 400 nm for 1.1- NA_{eff} to approximate 150 nm for 1.48- NA_{eff} , respectively.

The calculated results above show that the conventional detection of phase change medium (total intensity of x+y polarized) is from individual contribution of x and y polarization, respectively. Moreover, readout contrast in x and y-polarized are different functions of gap width. Since readout signal contrast from x-polarized is always higher than the sum, the readout signal contrast can be improved by filtering y-polarized. Taking $NA_{\text{eff}}=1.48$ full aperture objective for example, the intensity and contrast ratio of x-polarized/sum reveals a trade-off between signal improvement and detected intensity, as shown in Fig. 6. The x-polarized contrast is a factor 1.0 to 1.35 higher than the sum contrast at different air gap, at a cost of 0 to 25 percent total intensity reduction.

CONCLUSIONS

Comprehensive analyses based on rigorous vector diffraction theory have been presented to simulate the readout signal contrast using SIL optics in reading phase change recording disks. The readout signals of SIL-based systems are affected not only by evanescent coupling but also de-polarization effect in such high NA system. We noticed that the de-polarized reflected light (y-polarized from x-polarized incident beam) resulted in the reduction of total contrast, and became more seriously for high NA system. Moreover, more evanescent coupling will not contribute to signal contrast. Due to the signal degradation from de-polarized reflected light, a filtering de-polarized light is applied to signal detection. The reflected x-polarized contrast is a factor 1.0 to 1.35 times higher than the sum contrast (x+y polarized) at different air-gap, at the cost of 0 to 25 percent total intensity reduction.

Acknowledgement

This work was supported by National Science Council of the Republic of China under contract no. NSC 87-2622-E009-006.

Reference

1. E. Betzig, J. K. Trautman, R. Wolfe, E. M. Gyorgy, P. L. Finn, M. H. Kryder and C.-H. Chang, "Near-field magneto-optics and high density data storage," *Appl. Phys. Lett.* **61**, 142-144 (1992).
2. S. M. Mansfield, W. R. Studenmund, G. S. Kino and K. Osato, "High numerical aperture lens system for optical storage," *Opt. Lett.* **18**, 305-307 (1993).
3. B. D. Terris, H. J. Mamin, D. Rugar, W. R. Studenmund, and G. S. Kino, "Near-field optical data storage using a solid immersion lens," *Appl. Phys. Lett.* **65**, 388-390 (1994).
4. I. Ichimura, S. Hayashi, and G. S. Kino, "High-density optical recording using a solid immersion lens," *Appl. Opt.* **36**,

4339-4348 (1997).

5. Tom D. Milster, Joshua S. Jo and Kusato Hirota, "Roles of propagating and evanescent waves in solid immersion lens systems," *Appl. Opt.* 38, 5046-5057(1999).
6. M. Mansuripur, "Certain computational aspects of vector diffraction problems," *J. Opt. Soc. Am. A.*, 6, 786-805(1989).
7. Wei-Hung Yeh and M. Mansuripur, "Evanescent coupling in magneto-optical and phase-change disk systems based on the solid immersion lens," *Appl. Opt.* 39, 302-315 (2000).

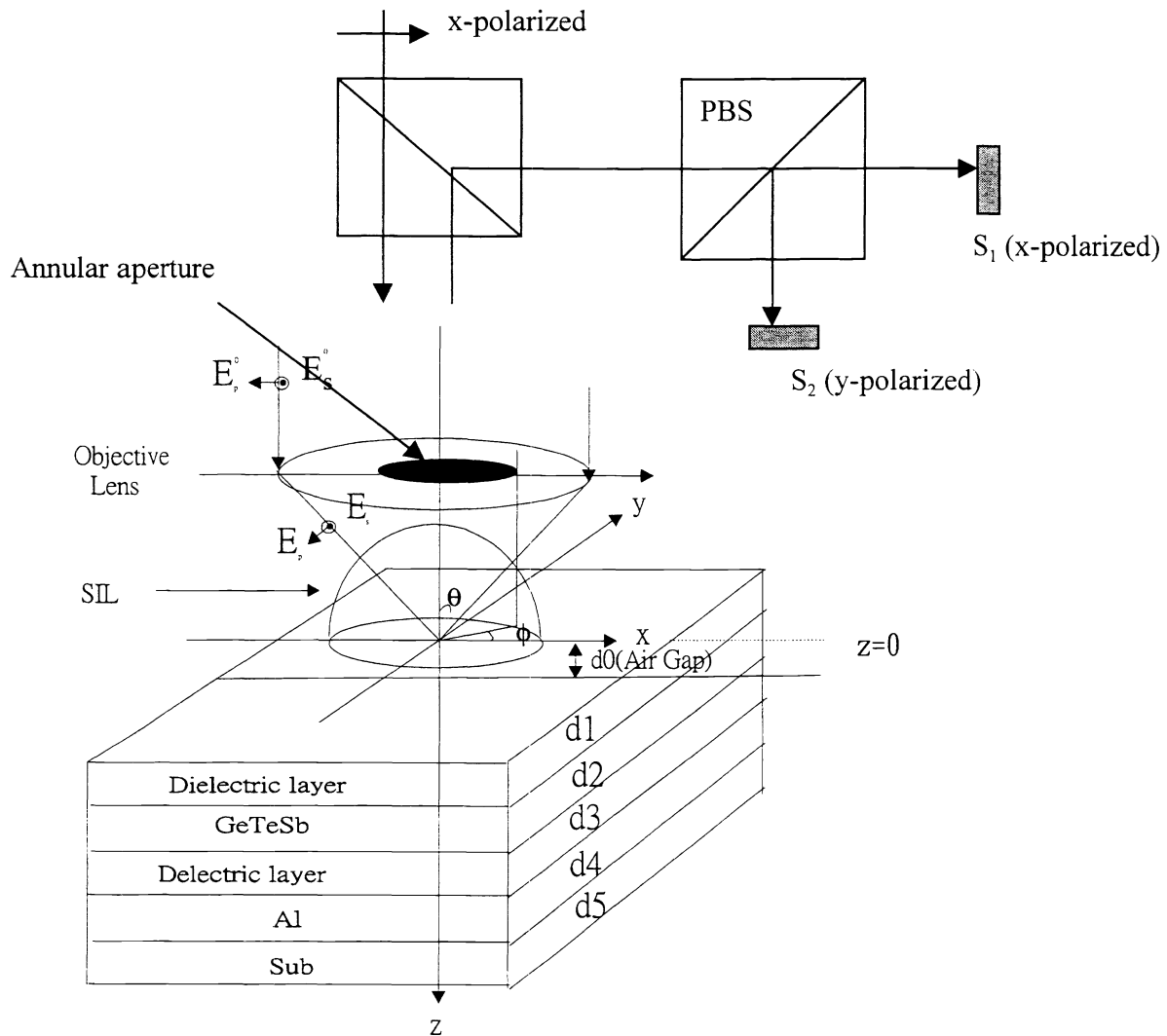


Fig. 1 Schematic of SIL-based system and disk structure.

($\lambda=650\text{nm}$, Focal length= 6000λ)

($d_1=110\text{ nm}$, $d_2=26\text{ nm}$, $d_3=32\text{ nm}$, $d_4=100\text{ nm}$)

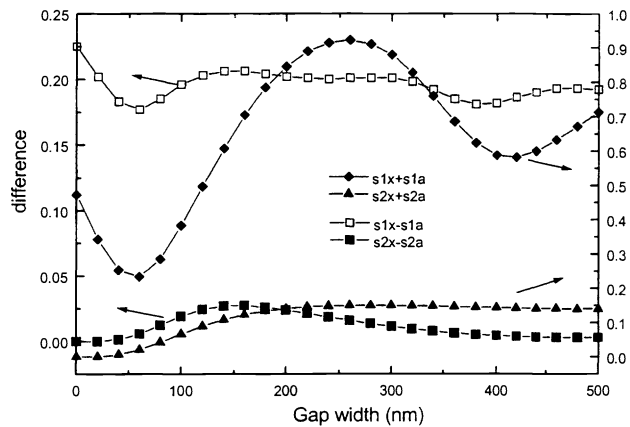


Fig. 2(a) Difference and DC values of x and y-polarized for the system of $NA_{eff}=1.1$, respectively. DC value of x-polarized ($S_{1x}+S_{1A}$) changes extensively as the gap width increases, which mainly determines the sum signal contrast $((S_{1x}-S_{1A})+(S_{2x}-S_{2A}))/((S_{1x}+S_{1A})+(S_{2x}+S_{2A}))$, as shown in Fig. 2(b).

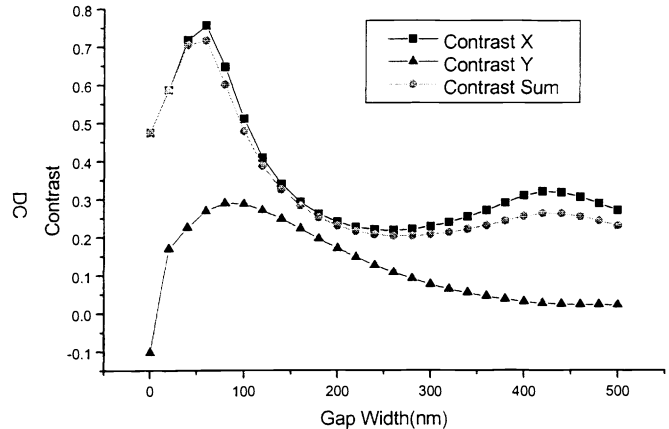


Fig. 2(b) The signal contrast in x, y, and sum (x+y polarized), respectively. The y-polarized reverses sign near gap width ≈ 0 nm, which result in total signal contrast reduction.

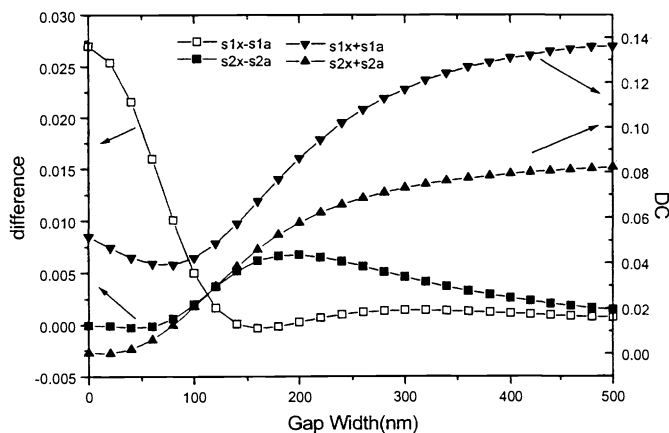


Fig. 3(a) Difference and DC values for the system of $NA_{eff}=1.1$ with an annular aperture blocking the rays below the critical TIR angle (evanescent wave). Both DC values of x and y-polarized increase as gap width increases because of total reflection effect.

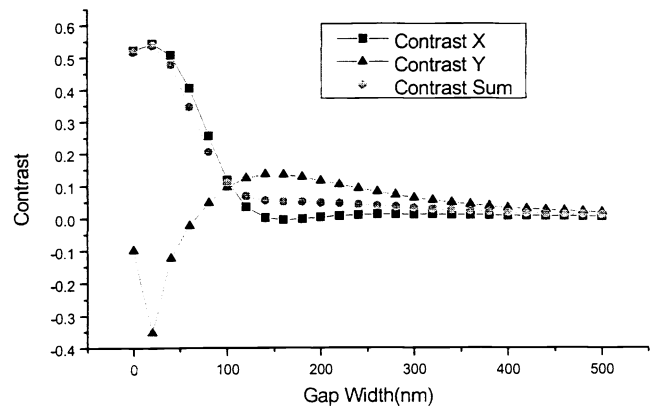


Fig. 3(b) The signal contrast with annular aperture in x, y and sum (x+y polarized), respectively. The contrast in y-polarized will make the total signal contrast enhanced or deteriorated. The contrast margin in sum is below 400 nm.

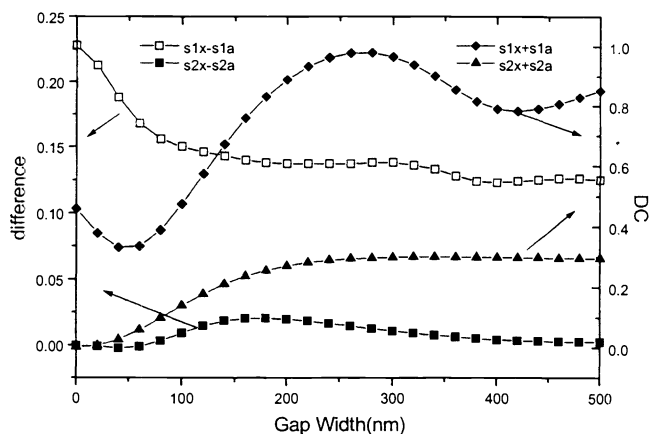


Fig. 4(a) Difference and DC values of x and y-polarized for the system of $NA_{eff}=1.48$, respectively. DC values in y-polarized increase compared to $NA_{eff}=1.1$ (Fig. 2(a)), result in apparent separation between sum signal contrast and x-polarized, as shown in Fig. 4(b).

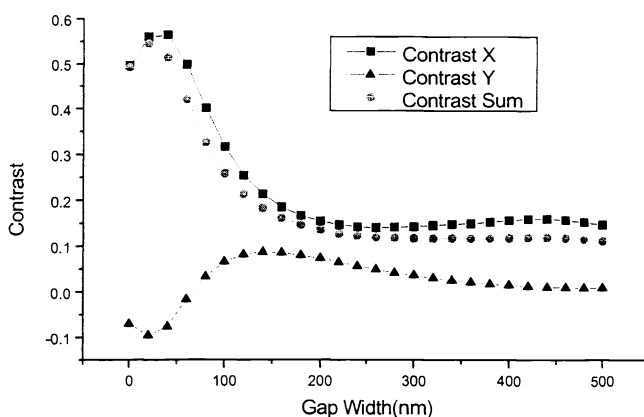


Fig. 4(b) The signal contrast in x, y, and sum (x+y polarized) for the system of $NA_{eff}=1.48$, respectively. The sum signal contrast is departed from x-polarized due to increased y-polarized.

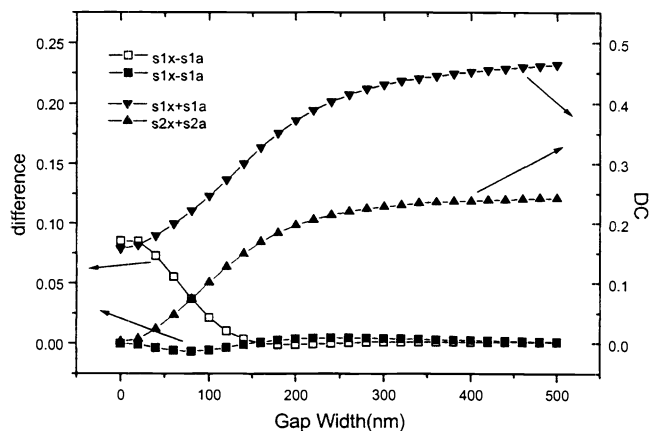


Fig. 5(a) Difference and DC values for the system of $NA_{eff}=1.48$ with an annular aperture blocking the ray below the critical TIR angle. Both DC and difference in x and y-polarized increase compare to $NA_{eff}=1.1$ (Fig. 3(a)).

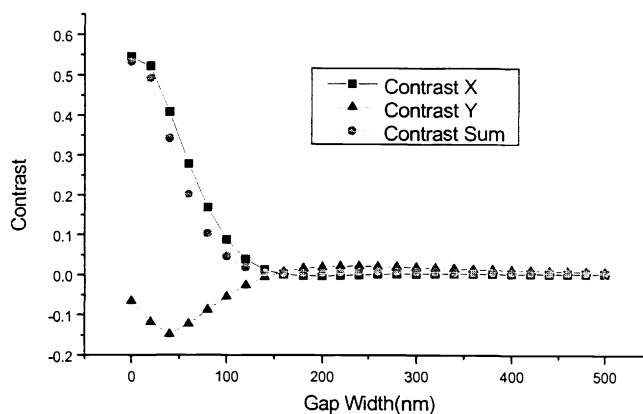


Fig. 5(b) The signal contrast of annular aperture in x, y and sum (x+y polarized), respectively. Signal drops more sharply than that of $NA_{eff}=1.1$ (Fig. 3(b)). Moreover, the contrast margin shrunk as gap is less than 400 nm in $NA_{eff}=1.1$ to approximate 150 nm.

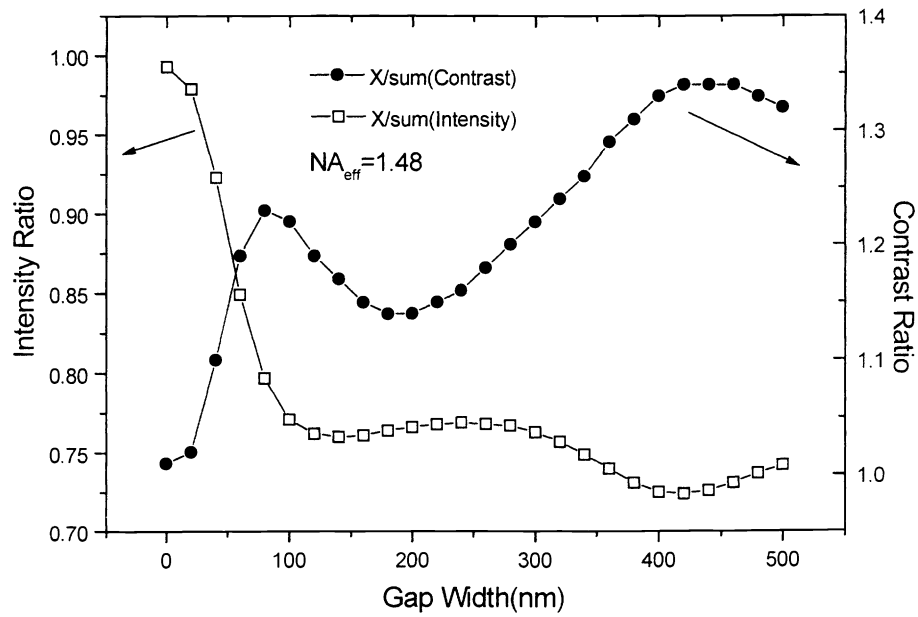


Fig. 6 Intensity and contrast ratio of x-polarized to sum (x+y polarized) for the system of $NA_{\text{eff}}=1.48$ with full aperture. There is a tradeoff between signal contrast and detected intensity.